COMITATO NAZIONALE PER L'ENERGIA NUCLEARE
Laboratori Nazionali di Frascati

LNF - 66/18
1 Aprile 1966

G. K. O'Neill : A MAGNETIC DETECTOR FOR ADONE. -

(Nota interna: n. 317)

Servizio Documentazione
dei Laboratori Nazionali di Frascati del CNEN
Casella Postale 70 - Frascati (Roma)

Laboratori Nazionali di Frascati del C.N.E.N.
Servizio Documentazione

LNF-66/18

Nota interna: n. 317
1 Aprile 1966

G.K. O'Neill[x]: A MAGNETIC DETECTOR FOR ADONE. -

In carrying out second-generation experiments at Adone, it will be necessary to have at least one general-purpose detector, subtending a large fraction of 4π in solid angle, and able to resolve all the known particle types which Adone is capable of making. As an initial goal this discussion assumes that the detector should be able to resolve the known particles when produced in two-particle reactions up to the full energy of the ring. By energy conservation it can then be argued that the momentum resolution of the apparatus will then be adequate for the study of more complicated multi-body reactions. The design of this detector, which has twenty-one cubic meters of useful magnetic field volume, was arrived at by consideration of a number of design criteria, the principle ones being:

1) For ease of scheduling, minimum interference with other experiments, and minimum lost time in the tuning of Adone, the detector should produce no magnetic field at the orbit of Adone; further, it should be so designed as to allow the convenient placement of higher-order correcting windings if necessary.

2) The detector should be compatible with a set of thin windows in the Adone vacuum chamber, and should itself interpose a minimum of material and a minimum actual distance between the source region and the region in which particle paths can be viewed.

3) Since experience with magnetic-field spark-chambers shows that a well-designed magnet will remain useful over the duration of many experiments involving radically different spark-chamber and trigger

---

(x) - Stanford Linear Accelerator, Stanford, Cal. (USA).

geometries, the magnet should leave a maximum volume free for experiments and should not be closely dependent on a particular spark-chamber geometry. Further, it should be conservatively designed as far as field is concerned, in case future needs dictate running it at up to twice the design field.

4) In spark-chamber experiments particularly when restricted by magnetic fields, either of analysis or storage-ring magnets, the field-lens and mirror systems usually become the most difficult parts to design, more so either than counters or the spark chambers themselves. Therefore if possible the detector should be usable with very simple optics (in the design discussed here there are no field-lenses or mirrors whatever in the main momentum-measurement views).

5) If possible the number of cameras required should be small, ideally one only, and the format should be simple.

6) The largest uncertainty in the design of experiments for Adone is the trigger rate that will be found in a given geometry. Therefore the design should place as few constraints as possible on trigger-counter geometry.

7) Beyond these special requirements, the usual ones of safety, initial cost, convenience and economical operation apply.

Many of the considerations which apply to this problem are identical to those of a detector studied in 1962 at the request of the builders of the 3 GeV storage-ring project at Stanford. That study is contained in an internal report[1].

Momentum resolution required

The whole energy of the circulating electrons in Adone is known to an accuracy of about 0.07% at 1.5 GeV[2]. With U the whole energy per particle, table 1 gives the momenta and the separations in momenta between charged particle pairs produced with U 1.5 GeV.

TABLE 1

Particle	Mass(GeV)	m/u	$(m/U)^2$	$\sqrt{1-(m/U)^2}$	p	$\Delta p/p$
Proton	0.938	0.624	0.39	0.78	1.17	
						> 17%
Kaon	0.494	0.330	0.108	0.944	1.416	
						> 5.4%
Pion	0.1396	0.093	$87(10)^{-4}$	$1-43(10)^{-4}$	1.496	
						> 0.18%
Muon	0.1057	0.0704	$49.5(10)^{-4}$	$1-25(10)^{-4}$	1.495	
						> 0.25%
Electron	0.0005	(0)	(0)	1	1.50	

Sigma and lambda pairs produced would decay within a few centimeters into products the charged members of which would always be particles within the table above. It is essential to have a high-resolution spark chamber very close to the beam to detect these decays.

It is not practical or necessary to provide within the available

space in an Adone experimental area a momentum resolution of 0.18%. The light-particle group (pions, muons and electrons) will therefore be separately identified by their interaction properties; such separation should be very good at 1.5 GeV. The momentum separation goes roughly as U^2, so at energies of a few hundred MeV, where interaction separation is not so clean, the magnetic analyser itself can distinguish members of the light-particle group. The crucial task of the magnetic analyser is to separate kaons from pions, both strongly-interacting.

To establish the momentum resolution requirements, compare the expected Kaon and pion cross-sections at 1.5 GeV. From p. 14 of ref. 2, with unity form-factors

$$\sigma(e^+e^- \rightarrow \pi^+\pi^-) \cong 0.25(10)^{-32} \text{ cm}^2 \text{ at } 1.5 \text{ GeV, and}$$

$$\sigma(e^+e^- \rightarrow K^+K^-) \cong 0.30(10)^{-32} \text{ cm}^2 \text{ at } 1.5 \text{ GeV.}$$

Assuming the nominal design-goal luminosity ($10^{33}/\text{cm}^2$-hour), there should be about three per hour of each of these reactions at 1.5 GeV, so that a 200 hour run would collect about 600 of each, giving 4% statistical errors in a cross-section. It seems reasonable therefore to require that the chance of misidentifying any single kaon pair as a pion pair, or vice-versa, be somewhat better, say 1%. 100 : 1 odds are reached at about 2.5 standard deviations (i.e., about 3.0 half-widths at half-maximum). Both product particles in each individual event necessarily have the same momentum, so each event gives us in effect two independent measurements of the same quantity. If each measurement has standard deviation a, the two measurements combined have a standard deviation $a/\sqrt{2}$. In our case the critical separation in momentum is 5.4%; so $a/\sqrt{2}$ is 2.2% and a itself, the required standard deviation on measurement of a single track, is 3,0%.

CALCULATION OF ERRORS IN MOMENTUM MEASUREMENT -

This section follows closely pp. 9-11 of ref. (1), but contains also a check of the formulas used against experimentally-observed resolution in a completed experiment using a magnetic-field spark chamber. The calculation is unsophisticated and makes an error of about 30% on the safe side.

The assumptions are:

1) Each track is measured at its end-points and at the center. Initially it is assumed that the space between spark-chambers is helium-filled; this will then be modified on the basis of the numbers. The length of track is taken as 1.7 meters, and the result can easily be scaled for other lengths.

2) The spark-scatter errors are equivalent to the use of 8-gap spark-chambers at the end-points, and a four-gap chamber at the center. The material of the chambers is equivalent to plates of thickness 0.025 cm of Aluminum; i.e., five such plates for the center chamber.

3) The chambers will be so arranged that track angles will be no more than about 45 degrees from the normal to the plates.

4) The scatter of sparks about the actual particle path has a standard deviation of 2.8 $(10)^{-2}$ cm. This is the value observed in the K_{e3} experiment[3] of P.T. Eschstruth, in which about two thousand e^+ tracks were analysed in a magnetic-field spark-chamber having twenty-four gaps of six mm. spacing (see p. 42, ref. 3).

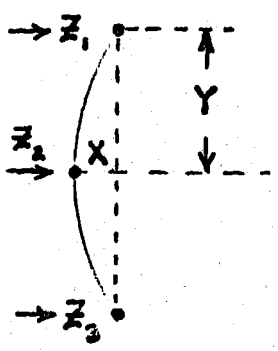

FIG. 1

In the figure 1, scattering at the endpoints Z_1 and Z_3 is neglected since it has little effect on the uncertainty in X, the sagitta.

If the track starts at Z_3 and ends at Z_1, Z_1 is uncertain both because of spark scatter ($\Delta Z_{1\text{-}s}$) and because of multiple scattering of the particle at the mid-point and in the gas ($\Delta Z_{1\text{-}m}$).

$$\Delta X = \sqrt{(\Delta Z_{1\text{-}s}/2)^2+(\Delta Z_{1\text{-}m}/2)^2+(\Delta Z_3/2)^2+(\Delta Z_2)^2}$$

The particle passes through only a small fraction of a radiation length, so is in the region of plural (Molière) scattering, and in traversing a thickness L will be scattered by a mean projected angle:

$$\text{Angle A} = (15/pv)\sqrt{L/L_{rad}}\,(1+b).$$ A is in radians, pv in MeV, L_{rad} is the radiation length, and for our case b is about -0.3. Then at an energy of 1.5 GeV,

$$A = 0.7(10)^{-2}\sqrt{L/L_{rad}}, \quad \text{and} \quad \Delta Z_{1\text{-}m} = AY.$$

With eight gaps at each end-point,

$$\Delta Z_{1\text{-}s} = \Delta Z_3 = 2.8(10)^{-2}\text{cm}/\sqrt{8} = 10(10)^{-3}\text{ cm}.$$

With four gaps at the Z_2 position,

$$\Delta Z_{2\text{-}s} = 2.8(10)^{-2}/\sqrt{4} = 14(10)^{-3}\text{ cm}.$$

The radiation length in Helium is 4200 meters, so the scattering in one meter of Helium is negligible even compared with that in $12(10)^{-3}$ cm of Aluminum:

$(L/L_{rad})_{\text{Aluminum}} = 12(10)^{-3}\text{cm}/8.86\text{ cm} = 1.4(10)^{-3}$. Therefore

$A = 0.7(10)^{-2}(3.7\text{x}10^{-2}) = 2.6 \times 10^{-4}$ radians, and $Z_{1\text{-}m} = 22\text{x}10^{-3}$ cm.

Combining these four sources of error in the sagitta,

$$\Delta X = (10^{-3}\text{ cm})\sqrt{(5)^2 + (11)^2 + (5)^2 + (14)^2} = 1.9 \times 10^{-2}\text{ cm.}$$

Apparently our choice of the number of gaps is not far from optimum, because the second and fourth terms in the square-root are nearly equal, and as the number of gaps N is increased the second terms goes as N, and the fourth term as N^{-1}.

In the spark-chamber design which turns out to be most convenient for installation and for photography, it will be a considerable further convenience if the entire region of the particle tracks can simply be filled with Neon. For one meter of Neon,

$L/L_{rad} = 2.6 \times 10^{-3}$, and the addition of the Neon changes the second term in the square-root to $(19)^2$, increasing ΔX by 28% to

$\Delta X = 2.4 \times 10^{-2}$ cm. The Neon is therefore tolerable although its effect is noticeable.

The sagitta required for the specified 3% momentum resolution is then $X = 2.4 \times 10^{-2}\text{ cm}/0.03 = 0.8$ cm. For the least favorable angles in the geometry under consideration, the track length is 1.6 meters. For this length and a momentum of 1.5 GeV/c, the required magnetic field is 2.5 kilogauss.

As a check on the expressions used in this section, they were applied to a completed experiment in which the momentum resolution (standard deviation) was known to be 1.8%. The calculation gave 2.6%, an overestimate. The more detailed calculation used by Eschstruth (Thesis, Princeton, 1955; PPAD 571 F) gave 1.9%, and is of course applicable to the case discussed here.

SCALING LAWS FOR MAGNET SIZE -

Our choice of magnetic field, and therefore of the linear dimension (scale size S) of the magnet, is limited by the need to keep the material near the interaction region thin, by the requirement of simplicity in photography, by coil power, and by the geometry of Adone. Within those limits though it is useful to consider several ways of scaling the magnet size:

1) Scaling with constant shaps, all linear dimensions proportional to S, with coil power held constant. In this case one can readily show that:

Field $B \sim 1/S^{1/2}$, resolution $p/\Delta p \sim S^{3/2}$, and so $p/\Delta p \sim \sqrt{\text{Cost}}$

2) Scaling with constant coil volume and constant coil power. Then the coil thickness $t \sim 1/S^2$, the coil resistance $R \sim S^2$, and for

constant power the current $i \sim 1/S$, so that $B \sim i/S \sim 1/S^2$. Then the sagitta X = constant, and the magnetic flux to be piped is also constant, so that the volume and cost of iron are proportional to S. Summarizing, in this method of scaling the momentum resolution, the coil power, the cost of the coil and the total magnetic flux all remain constant. The cost of the iron goes only as the first power of S, and the coil thickness decreases as S^2.

With these two scaling rules one can then arrive at a good choice of scale in a logical way. (1) shows how the cost depends on the momentum resolution demanded. (2) shows how, everything else kept constant, the coil thickness depends on the cost of the iron in the magnet. In the present case the coil volume is set by the requirement that the power be kept near 1 Megawatt. The design which is favored leaves the Adone orbit field-free by providing current sheets above and below the interaction region. By rule (2) the thickness of the coil can be made as small as desired by increasing the scale size S, the overall magnet cost changing only rather slowly as S is increased. The design choice made in the next section holds the coil thickness near the interaction region to 0.08 radiation length. An optimum final choice would probably lie in the region $0.6 < S < 1.2$ of the linear size chosen here. The corresponding range of magnetic fields is 1.75 to 7.0 kilogauss. Those numbers are quite consistent with those which have been found by experience to be the most practical for magnetic-field spark chambers.

MAGNET GEOMETRY -

The figure 2 is a section seen from the side of Adone, looking along a line perpendicular to the orbit at the center of an experimental straight section. The approximate positions of the Adone quadrupoles are shown, and the section is taken through the iron of the return yoke. The Fig. 3 is a section taken at the center of the straight section, looking along the orbit of Adone.

The coil consists of a single-layer winding of 1 cm x 5 cm Aluminum conductor, with a 6 mm diameter water hole at its center. There is only one shape to be wound, and presumably it would be most convenient to have the single layer made up of pancakes 10 cm or 20 cm thick. Upon completion of the winding, the completed pancakes are then simply milled to form a shape indicated in fig. 3. The coil surrounds and protects the thin window in Adone; on the outer side the milling of the coil is continued from end to end, to provide for simple photography of the high-resolution spark chambers or streamer chambers near the interaction point. The bends in the coil are all circular arcs, of minimum radius 25 cm. There would be no joints in the conductor except at a convenient manifold-point indicated in fig. 2. The shape has been made a little more complicated than presently needed, in order that a maximum space along the orbit of Adone could be made usable later if desired. For the same reason two small sections of iron in the re-

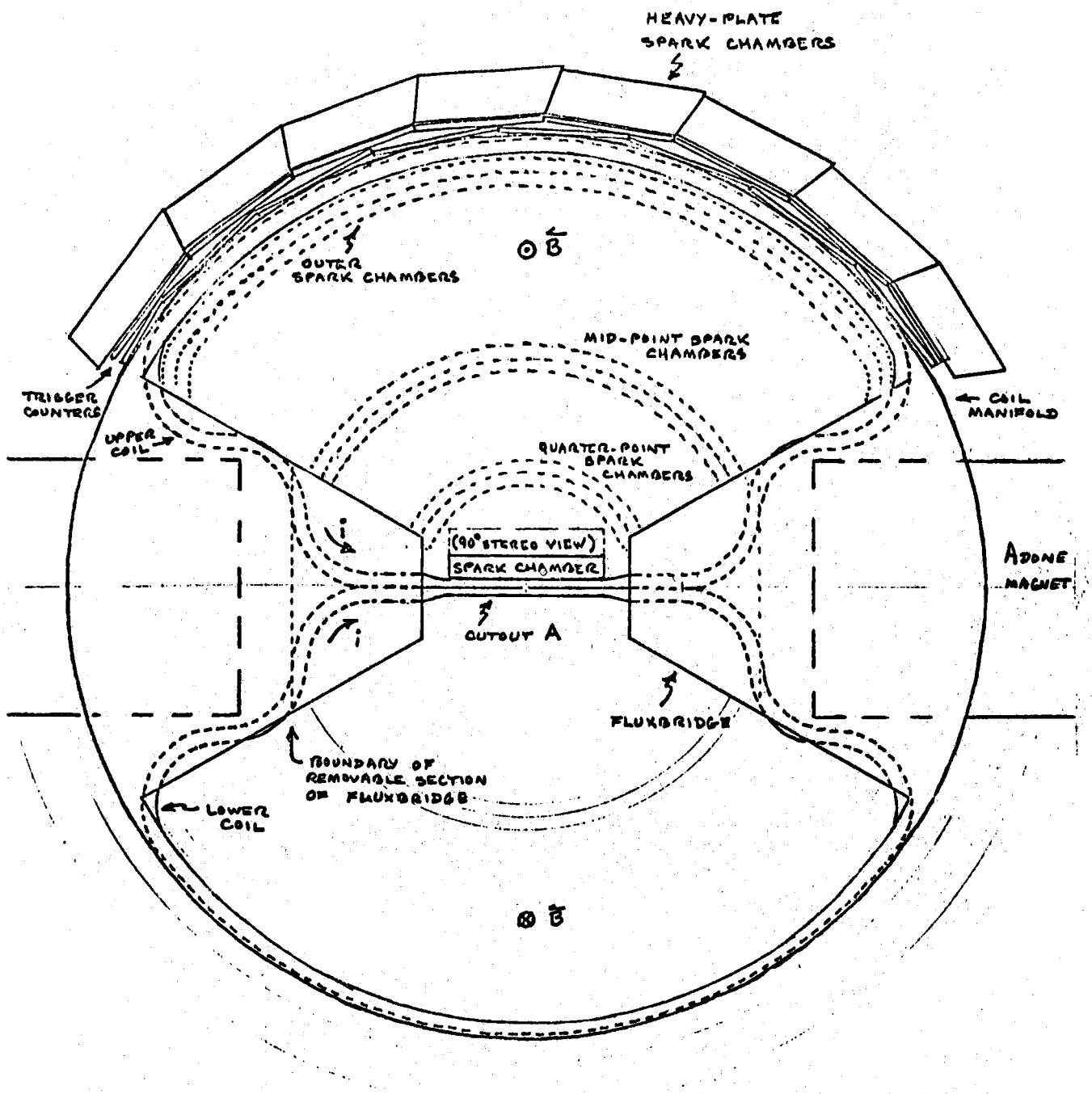

NOTE: APPARATUS DETAILS BELOW THE MEDIAN PLANE ARE SAME AS THOSE ABOVE MIRROR-IMAGED.

FIG. 2

turn yoke are to be removable.

For particles of the full 1.5 GeV/c, and for a fiducial beam--source length of 10 cm, the coil leaves free half the azimuthal angle, and a region down to 30 degrees in projected polar angle. Simply by adding additional identical coil sections, with no changes in the magnet yoke, one could make the azimuthal coverage as large as desired.

The coil currents are symmetric on reflection in the median plane of Adone. The basic magnet symmetry therefore insures that on the orbit of Adone there is no magnetic field component except a vertical one. In the yoke design shown in fig. 4, photography is assumed to be from one side only, and the field is maximized by having a simple one-piece disc, 25 cm thick, as the return yoke on the side not viewed. If the yokes were identical there would be no magnetic field at all on the Adone orbit; as it is there may be a small residual vertical field, which could be reduced to zero by some shaping of the iron or by providing in the magnet itself a small correction winding which could be laid flat on the coil surface or located at the interface between the two halves of the coil.

If one end of the coil were not left partially open, the field would be uniform throughout and its direction would be everywhere parallel to the coil axis. As it is there will be some effect due to the partially-open end, but the field will be nearly uniform in the regions most important for momentum measurement. Even with the asymmetric yoke the magnet will have no dipole field component; the field outside it should be close to zero, and at long range it will fall off as a quadrupole field.

Because in this coil design the lower coil acts as the return-yoke for the upper, no flux need be piped by the iron from end to end of the coil. The outside of the coil can therefore be entirely exposed, so that there is no restriction on the placement of trigger counters and heavy plate spark chambers. The same property makes it possible to extend the magnet along the field axis at any future time by the addition of coil sections. The magnetic field has been held to 10 kilogauss maximum in the iron. To check for any weak points in the magnet design it will be convenient to build a small-scale model magnet. At low fields, in fact, it will be sufficient to model only half the magnet, replacing the entire region below the median plane by an iron sheet, since the magnet symmetry forces the median plane to be a magnetic equipotential. In the same way, it is instructive to visualize the magnetic field shape (see fig. 4) by imagining that the magnet is sliced in two along the median plane of Adone, and that the median plane is then replaced by the surface of an iron table. In the approximation of infinite permeability all the iron of the magnet, although divided into two pieces, is at the same magnetic potential.

Coil specifications:

Material: Aluminum, cross-section 1 cm x 5 cm with centered water pas

Conductor Cross-section At Center of Interaction Straight Section.

Effective length of coil:

Cutout A is the full length of the coil, i.e. 3.0 m transverse to the beam; it increases the effective length of the coil by 60 cm (2/3) = = 40 cm.

Cutout B is 15 cm transverse to the beam; that 5% of the coil has its effective length increased by 150 cm (2/3) = 100 cm.

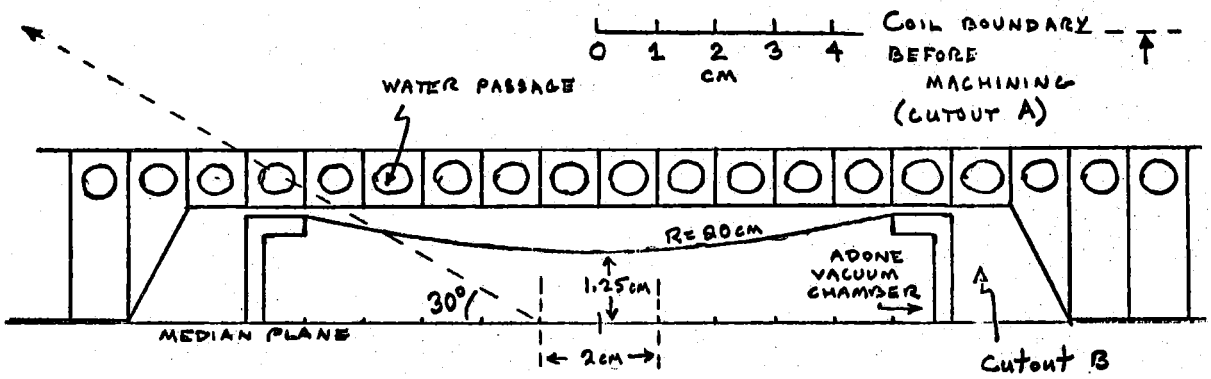

Material along particle path:

Thin window in vacuum chamber: 10 cm wide, 0.05 cm thick (0.03 radiation length in stainless steel). Stress = 5,500 psi = 370 Kg/cm^2.

Current sheet of magnetic detector:

At 90 degrees: 0.75 cm Aluminum = 0.085 radiation length = = 0.025 collision length.

At 30 degrees: 1.5 cm " 0.17 " " = = 0.25 coll. len.

First-view distance: 3 cm from center of interaction region.

Azimuthal angle limit: $\Delta\phi = (2/3)(2\pi) = 240$ degrees. This limit is (for short tracks) mainly due to the limited size od a thin window for the vacuum chamber; a different vacuum chamber design could make use of a wider cutout B.

FIG. 3

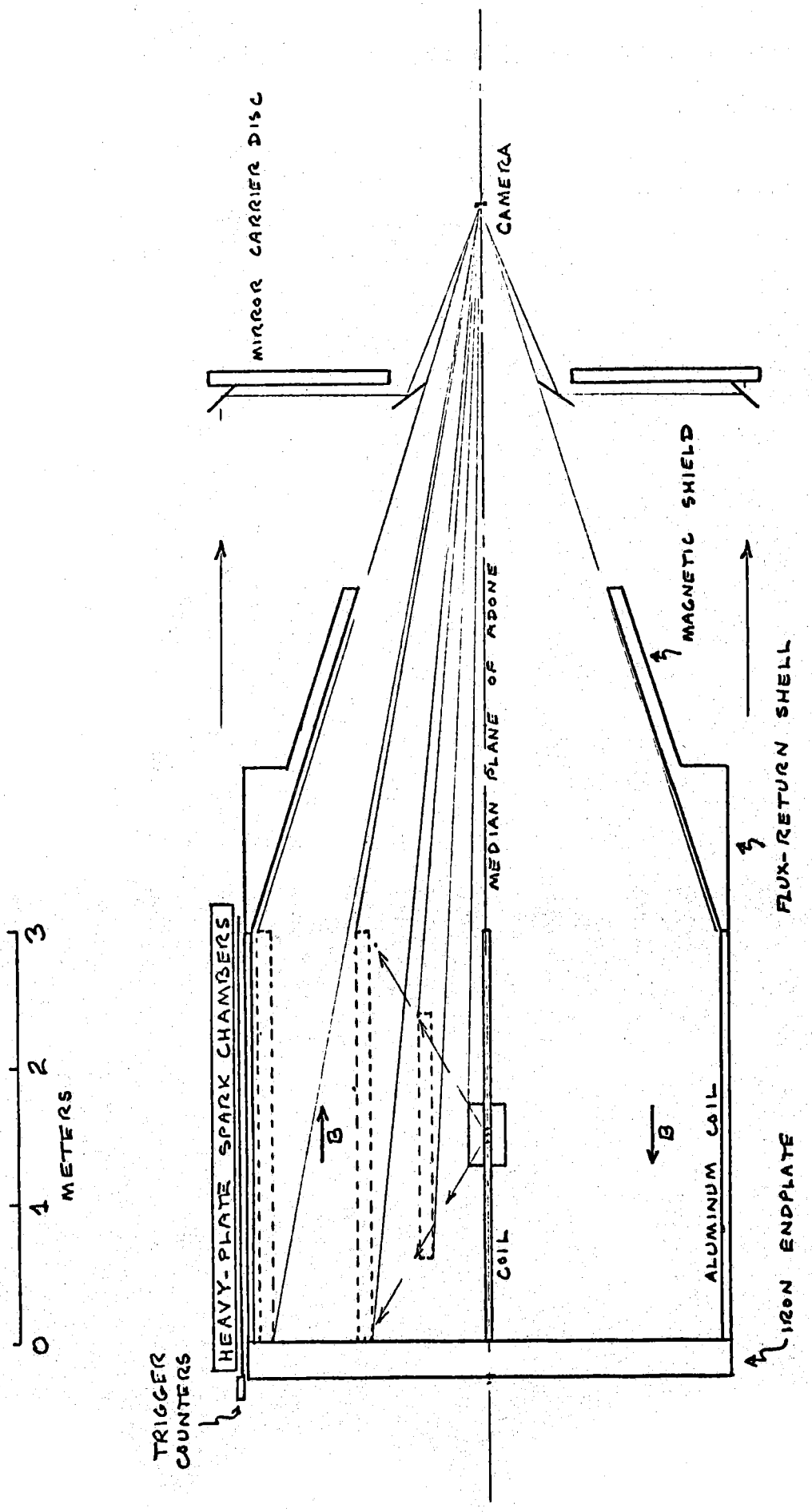

FIG. 4

VIEW PARALLEL TO BEAM

ge.
Total length both coils per turn: 15.0 meters.
Effective length increase, both coils, per turn, due to outout A: 5.3%
Effective length increase, both coils, average over entire winding, due to cutout B: 0.7%.
Effective total length of coil: 15.9 meters.
Resistance regarded as a pair of single turns in series: 3.00×10^{-6} ohms.
Current density: 2,000 amperes/linear cm.
Total power: 1.08 megawatts.
Total weight of coils: 6.7 metric tons before machining.

Iron specifications:

Endplate: Disc, 3.5 m diameter, 0.25 m thick. Flamecut plate.
19 metric tons.
Shell: Cone, 3.5 m outer diameter, cylindrical symmetry. Sandcast
27 metric tons.
Shield: Cylindrically symmetric. Sandcast
6 metric tons.
Bridges: Trapezoidal, 0.2 m thick. Flamecut plate.
4 metric tons.
Total weight of iron: 56 metric tons.
Note: Flux paths are entirely within single pieces of iron, so no machining is necessary after flamecutting or sandcasting.

SPARK CHAMBERS AND PHOTOGRAPHY -

As noted in the introduction, the problem of field lenses and mirror alignment is usually more troublesome than that of spark chamber construction. Furthermore the number and complexity of fiducial markers necessary when many views have to be combined is great. In the present case the magnet design chosen is entirely compatible with the use of conventional multiplate spark-chambers, but there is another way of solving the problem which seems to have many advantages: uniformity of efficiency over projected polar angle, freedom from any fiducial cuts in polar angle, single-camera photography of both coordinates in a single view, and preservation of the real-space pattern for easy scanning. Furthermore, this solution would require no field lenses or mirrors in the momentum-measuring views.

The solution proposed is simply to use, for the middle and end-point spark chambers, two-gap wire-grid chambers of moderately large gap spacing (5 cm), and to use a single camera placed on the symmetry-axis of the magnet. (See fig. 4). Wire-grid spark chambers have already been used successfully at CERN in a beam profile monitor. Those required for the experiment under discussion would be made up of 0.01 cm wires, spaced 0.15 to 0.20 cm apart, and all would run parallel to the magnet axis. The choice of gap spacing (5 cm) is made to

insure that any distortion of the sparks due to the finite wire spacing would be confined to a few percent at the ends of the sparks, so that good measurements could be made over most of the length of the sparks. There would be no cross-wires, and the geometry could be maintained quite accurately and simply by putting tension on each wire. These chambers would operate in the spark mode, not the streamer mode, and should give very bright tracks. Since they can be made cylindrical (which would be very difficult by conventional methods over such large dimensions) the maximum angle to the normal which any individual track would make is only 45 degrees for the end-point chambers.

These chambers would be transparent and so could be viewed through their plates. A momentum measurement would consist simply of a measurement of projected polar angle in each chamber; this is exactly the same angle that the spark image would have on the film format. The radius of the spark image from the center of the film format would be in 1:1 correspondence with the spark position along the magnet axis; the corresponding stereo angle would be fairly good: 1 in 4, on the average, for the outer chambers. This would yield a dip-angle measurement of about 0.6 mm/1.5 meters, or 0.5 milliradian. To keep the film format simple, one chamber would not be viewed through another.

Close to the interaction region there would be chambers above and below, viewed by the same camera that would view the wire chambers. Probably these starting-point chambers would be multiplate with 6 mm spacing, for high space resolution, the resolution of V-decays, and for good efficiency on low-momentum tracks at large angles to the plate normals. Although no mirrors would be used on these chambers for the front views that go into the momentum measurement, several would be used to give 90 degree stereo and to give additional views not partially occulted by the thin edge of the magnet coil.

Outside the coils, at a 1.55 m radius, there would be heavy-plate spark chambers, probably using copper-plated iron plates. Only one view need be taken of these chambers because measurements in them would consist simply of spark counts in each gap. They can be viewed, again by the same camera, in a way which preserves the real-space format. In that way a scanner could tell at a glance whether a given track in the momentum chambers was a pion, muon or electron. For simplicity and freedom from maintenance problems on mirror alignment, all the mirrors required for the heavy-plate chambers would be carried on a single carrier-disc, shown in fig. 4. The chambers would be conventionally made with lucite or polyvinyltoluene frames; in their front views they would be stacked not in rectangular outline, so that they would not have fiducial edges. They would incidentally serve as magnetic shields against small residual fields escaping from the coils.

Electrical drive for spark-chambers: it would be convenient and effective to drive the chambers through cables, from an annular ring at one end, and to place terminating resistors on the annular ring supporting the other end of each cylinder; i.e., the chambers would be driven like 3 m lengths of cylindrical coaxial cable, terminated in the correct characteristic impedance. In the summaries which follow, it turns out that all of the chambers for the entire detector could be driven from a pulser which already exists at Princeton and which has been successfully used in one experiment. This pulser can provide 50 kilovolts into each of 64 50 ohm cables, with a risetime of about 15 nanoseconds.

Spark chamber specifications:

Inner (starting-point) chambers: 6 mm gaps, thin plates, area 46 cm x 60 cm, height 10 cm.
End-point chambers: Area 20 m^2 each gap. Total capacity 8,000 picofarad.
Impedance 1.25 ohms. Drive from 40 cables (RG9/U) at 50 kv to give 10 kv/cm.
Mid-point chambers: Total capacity 4,000 picofarad. Impedance 2.5 ohms.
Intermediate (quarter point) chambers: capacity 1,000 picofarad.
Heavy-plate chambers: 6 gaps of 1 cm each. 1 cm iron plates. Total 7 radiation lengths, 1.0 collision length. Total weight 23 metric tons. These chambers could be made thicker as required. Total capacity = 2.3 x x 10^4 picofarad.

Camera and film format:

The object distance is 5.3 m to 8.3 m, and the object has a diameter of 3.8 m.
The diameter of the circle of confusion due to depth of focus is, on reprojection,

$d = \Delta p / M f$, where Δp is the distance of the object from the center of focus, M is the demagnification, and f is the f-number of the lens. The formula above overestimates the size of the circle of confusion by a factor of roughly two. Experience indicates that there is very little loss in accuracy of measurement if d as given by the formula above is allowed to be 2 mm. The possible choices of film size and f-number include:

70 mm film, 60: 1 demagnification at f:26 (60 mm format diameter)
35 mm film, 120:1 demagnification at f:12 (30 mm format diameter)
35 mm film, 150:1 demagnification at f:8 (24 mm format diameter)

The second example quoted corresponds to unperforated film, the last to perforated film. The best choice may well be the last, since modern films have very fine grain if the speed requirements are not excessive. That choice would permit the use of the very reliable Flight Research camera, which can transport 20 frames/second asynchronously, can accept 1,000 film magazines, and has a vacuum hold-down. One such camera will be available on completion of the colliding-beam experiment at Stanford.

CHOICE BETWEEN CONVENTIONAL AND CRYOGENIC COILS -

To check whether a cryogenic coil would be preferable to the conventional coil assumed so far, a comparison of costs will be made, based on the latest available information on available superconductors, as supplied by Brechna in a seminar given at SLAC. A stabilized design is assumed; this is one in which the superconductor is parallelled by sufficient copper so that in the event of a local warmup the conductor will recool reversably, rather than going to the normal state instantaneously and regeneratively. A 2,000 ampere cable has a diameter of 0.7 cm and is about 40% Nb-Ti, 60% Cu strands. A single-layer coil with 70% packing would do the job. Its total length would be 15 m x 300 turns 4500 m, and the cost of the cable, not yet wound, is estimated as $ 30,000. The other costs listed below are taken from Brechna's engineering study of a coil of very similar size and surface area.

Superconducting coil; capital costs:

- Cable (raw-material cost)	$ 30,000
- Dewar	$ 18,000
- Helium refrigerator	$ 42,000
- Power supply for turnon	$ 10,000
- Cable winding cost	$ 48,000
- Total cost for cryogenic system	$ 148,000

Operating cost: The estimated heat load requires about 20 liters/hour of liquid-helium refrigeration, and on each cool-down some hundreds of dollars worth of liquid helium would be required. Presumably the salaries of at least one or two men as cryogenic technicians would be required.

Room-temperature coil; capital costs:

- Conventional Aluminun coil, wound	$ 66,000
- Power supply, 1.08 Mw $ 60/kw	$ 65,000
- Cooling tower capacity at $ 30/kw	$ 27,000
- Total cost for conventional system	$ 158,000

There are probably more hidden extras in the cryogenic coil, but superficially the capital costs are about the same either way. The operating cost of the conventional coil would be $ 11/hour at 1¢/kwh. For a 200 hour run the conventional coil would therefore cost $ 2,200 to $ 4,400 to operate, depending on local power costs.

On balance, the operating costs of the cryogenic coil would probably be a good deal higher because of the technicians' salaries required. At the large bubble-chamber installations where cryogenic coils are now popular there already exist large staffs of such technicians. The main disadvantage of the cryogenic coil, however, is that it needs to be surrounded by 5 cm of insulation and liquid-nitrogen jacketing, which makes

it awkwardly thick. If the coil power were an order of magnitude larger, however, the best choice might well turn the other way, in spite of the short radiation length in Nb-Ti.

ANALYSIS BACKGROUND -

The momentum analysis provided by the magnetic detector will distinguish real events from any caused by particles lost from the A-done beams. Even without such analysis the geometrical resolution provided by spark chambers would make it almost impossible for a spillout event to duplicate a colliding beam event. However, cosmic ray muons will constitute a background which must be calculated.

Integrating over all angles, the cosmic ray muon background at sea level is 1 particle/cm^2-minute, in a spectrum which has an effective width of about 3 GeV. In a 2.5% momentum window at 1.5 GeV/c, there are about 1.2% of all muons; that is, the magnetic analysis alone gives a rejection ratio of 80. In Adone, the RF frequency is 8.58 Mc, so for an RF-linked gate window of 5 nanoseconds there will be a rejection factor of 117 ns/5 ns = 23. It will be helpful to have an additional rejection factor of the order of five. This can be achieved by using time-of--flight. The large trigger counters are separated by 1.7 m x 2 x 3.3 ns/m = 11 ns. They can be 2.5 cm thick, 50 cm wide, and 3 m long in the direction of the magnet axis, viewed by a single tube. If the tubes for the top counters are located at one end of the magnet, and those for the bottom counters are at the other end, all particle pairs produced by the colliding beams, at any angle, will be in exact time coincidence, including the effect of the finite transit time of the light in the scintillators. The display of pulse arrival time for a large number of counters is a relatively inconvenient solution to the problem, at the present state of electronics, and it would probably be simplest to require time-coincidence between upper and lower counters, with a coincidence full-width of 10 ns. Assuming for the Adone beam a fiducial source area of 2 cm wide by 10 cm long in the median plane, the cosmic-ray background within the fiducial area will then be

$$(1/cm^2\text{-minute})(1/80)(1/23)(1/5)(20cm^2)(60\text{min./hr.})=0.13/\text{hour}.$$

For electron-positron annihilation into muon pairs, LNF-65/25 quotes a cross-section of 10^{-31} cm^2 at an energy of 424 MeV, for unity form factor. The cross-section goes as E^{-2}, so at 1.5 GeV we expect for muon pairs 8×10^{-33} cm^2. Taking the nominal quoted luminosity for Adone, the yield is

$$(10^{33}/cm^2\text{-hour})(8\times10^{-33}cm^2)(1/2)=4 \text{ events/hour for the solid angle}$$

of the detector design discussed here. The cosmic-ray background would

then be about 3% if the muon form factor is unity and the luminosity of Adone is as expected.

TRIGGER COUNTERS -

The requirements on trigger counters are by far the most uncertain item in the detector design, but for the present it is assumed that there will be at least a six-fold coincidence:

32 counters of 50 cm width by 300 cm length, forming two layers just above the upper coil and two layers just below the lower coil. The layers would be staggered and, to avoid edge-fiducial problems, a coincidence would be accepted between a counter of the lower bank and either of two adjacent counters in the upper bank.

Two very thin counters above and below the interaction volume between the coil and the first spark chamber. These would have an area just large enough to include the angular acceptance limits.

TRIGGER RATES -

The triggering rate to be expected in a given configuration of counters, magnetic fields, and shielding is very difficult to calculate, although perhaps not impossible with the help of the fastest computers now in existence; the major difficulty is that the rejection ratios required are so large that a very large number of Monte Carlo trials must be made before even one trigger event is found. In this section a relevant example is discussed, a comparison of it to Adone is made, and a method of obtaining the trigger rates accurately in advance of completion of Adone is described.

In the electron-electron experiment as operated in 1965, triggering was by a six-fold coincidence of counters all 6 mm x 25 cm x 50 cm in size, arranged in groups of three with spacings of 4 cm, the groups being 25 cm from the center of the interaction region. There were four spark chambers, interleaved between the scintillators, so that one can make definite statements about the kind of events that caused triggers. There were four classes, each accounting for about a quarter of the triggers:

1) Track visible in upper chambers, lower counters triggered by photons.

2) The same but with the roles of upper and lower reversed.

3) Tracks visible in upper and lower chambers both, apparently coming from a point near the end of the interaction straight section.

4) No visible tracks; counters triggered by photons only.

In all cases where there was a visible track, the apparent origin of the track was, as expected, in the vicinity of the end of the interaction region.

With typical operating conditions at 300 MeV, the beam intensities were 30 ma each ($8x10^9$ electrons) and the lifetime was roughly half an hour. The loss rate was therefore

$8x10^9/10^3$ seconds = $8x10^6$ particles lost per second, and in the 1 meter region just upstream of the interaction section there were, for both beams together, about 1.6×10^6 electrons lost/second. Under these conditions the six-fold trigger rate was about 1 trigger/10 second. The rejection factor for the system was therefore 1.6×10^7. It is known from earlier tests that an additional pair of counters, giving an eight-fold coincidence, would have reduced the trigger rate by about another factor two.

Fortunately there will shortly be more information on trigger rates, because during March and April 1966 a new set of much larger counters, giving a ten-fold coincidence and including a set of small counters close to the interaction region, will be tested at 300 and 500 MeV. From these tests a good deal should be learned about scaling both in counter size and in energy.

The expected numbers for Adone are quite similar to those for the electron-electron experiment. At the nominal beam intensity (92 ma) there will be 2×10^{11} particles stored in each beam. The circumference is 105 meters, and from this larger storage ring and effective source region of 2 meters is reasonable. Given a beam lifetime of 10^3 seconds, the number of particles lost per second in the most important 2-meter region will be

$2 \times 10^{11} x 2x(2 \text{ meters}/105 \text{ meters})/10^3$ second = 8×10^6/second. This is about a factor five higher than for the electron-electron experiment, and the energy is also higher. In a 200 hour run we cannot tolerate scanning more than about 10^6 pictures, so the tolerable rate of triggering is at most about 1/second. The required rejection ratio is therefore 8×10^6, a factor of five better than has so far been achieved in the elctron-electron experiment. If the spillout background at Adone is uniform in time, roughly a factor ten can be gained by taking a 10 ns coincidence with the RF system.

In 1963, before installation of counters at the electron-electron experiment, a mock-up was made of an interaction region with its adjacent storage-ring magnets, and a beam of a few hundred electrons per pulse from the linac was brought into the magnet and made to dump just upstream of the counters. It is from these tests that it was concluded that counters could be located very close to the vacuum chamber. It might be well worthwhile to set up at the Frascati synchrotron a scattered-beam facility, in which about 10^3 electrons per pulse, energy analysed and in a tight beam, could be brought to a small experimental location where mockups of proposed Adone triggering systems could be located. In such a beam runs of half an hour would be enough to establish triggering ra-

tes with the rejection ratios that are required for Adone, and such a facility would in particular be quite useful in the design of trigger counters and logic for the magnetic detector. If it is impractical to make an arrangement the tests will have to await the completion of Adone.

COSTS -

Much of the cost of the magnetic detector will be in the form of continuous materials and salary expenses for the group that will build it, but it is worth estimating roughly the costs of some major items. In the following list this is done both for the design described in this report, and for the same design scaled linearly by a factor $1/\sqrt{2}$, that is to a track length of 114 cm.

Item	Total req.	Assumed unit cost	Design as described	Scaling law	Scaled design
Magnet iron	56 met. tns.	$2/kg	$112k	S	$ 79k
Magnet coil	6.7 " "	$10/kg	$ 67k	Const.	$ 67k
Power sypply	1.08 Mw	$60/kw	$ 65k	Const.	$ 65k
Cooling t'r.	1.08 Mw	$30/kw	$ 33k	Const.	$ 33k
Sp.Ch.iron	23 met. tns.	$3/kg	$ 69k	S^2	$ 35k
Trig.Scint.	1.12 m^3	$.05/cc	$ 56k	S^2	$ 28k
Pm tubes	50	$0.5k	$ 25k	Const.	$ 25k
Elec. Ccts.	160	$0.4k	$ 64k	Const.	$ 64k
			$491k		$369k

Thes cost estimates are very rough and should be replaced by more responsible ones; in general an attempt has been made to put them on the safe side.

REFERENCES -

(1) - G.K. O'Neill, "Analysis of reaction products from e^+e^- at 6 GeV (CMS)", August 1962, SLAC. TN-62-41.
(2) - R. Gatto, "Theoretical aspects of colliding beam experiments". LNF-65/25, (1965) (See esp. pp. 14 and 26).
(3) - P.T. Eschstruth, "Positron momentum spectrum from K^+_{e3} decay". (Thesis). PPAD 571 F, October 1965.
(4) - (General Reference): "Adone - The Frascati 1.5 GeV Electron-Positron storage ring", LNF-65/26, (1965).

APPENDIX -

CHOICE OF MAGNET GEOMETRY -

Analysing magnets for storage rings can be divided into two classes: those which affect the particle orbits in the rings and those which do not. Those in the first class can be used either with the addition of nearby compensating fields, or by a realignment and repowering of the storage ring bending magnets so that the analysing magnet provides part of the bending for the storage ring particle orbits; the latter alternative opens the possibility of an increase in the effective straight-section length, as well as clearing the median plane and the region near the vacuum pipe of any excess material. For that reason it will probably be the ultimate solution after some period of storage-ring operation. Initially however it will probably not be highly popular with those responsible for making the storage ring work, and for that reason this discussion will concentrate on magnets of the second class, which, as self-contained units, have zero dipole field and zero or small fields of low multipole order at the particle orbits.

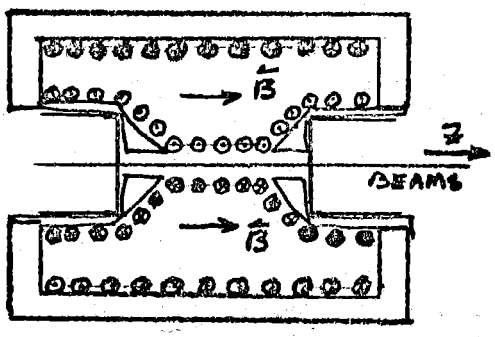

1) Compensated solenoid: In this design, in which the coils are symmetric in rotation about the particle orbit, if the axial direction is z both the inner and outer coils must satisfy a current-sheet condition $di/dz = \text{constant}$, the same constant for both inner and outer coils. There need be little or no stray field, and the currents required are not excessive anywhere. The magnetic field is uniform throughout its entire volume, and is in the z direction. There are three principle disadvantages to this design: the structure topologically links the storage-ring vacuum chamber, so that work on the spark chambers, mirror alignment, etc., can only be done in place or by opening part of the ultrahigh vacuum chamber. Second, photography is rather difficult and requires either several cameras or a very elaborate mirror and lens system. Third, in the circular version the "first-view" distance from the orbit to the first spark chamber is larger than would otherwise be necessary. In practice this geometry would be most useful distorted into ellipsoidal rather than circular cross-section; it would be worth looking into the variant which might preserve the Cauchy conditions and the uniformity of surface current density. Inherently this design, which has very low analysing power for particles of low polar angle, is not badly suited to the expected angular distribution for electron-positron reactions.

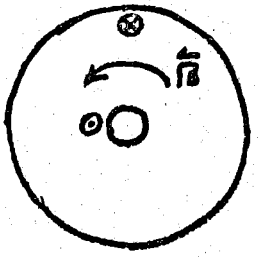

2) Coaxial conductors: This geometry is free of the first two disadvantages of the previous example. Its major disadvantage is that the current density required for the center conductor is excessive. Like the

first example, it would be more useful in a distorted version which would reduce the first-view distance. Its analysing power would be a maximum for particles of low polar angle, and its magnetic field would be non-uniform. By a process which is amusing to consider topologically (see steps below) it can be turned into geometry (3), which is the one considered in detail in this report.

Steps in transformation of geometry (2) into geometry (3):

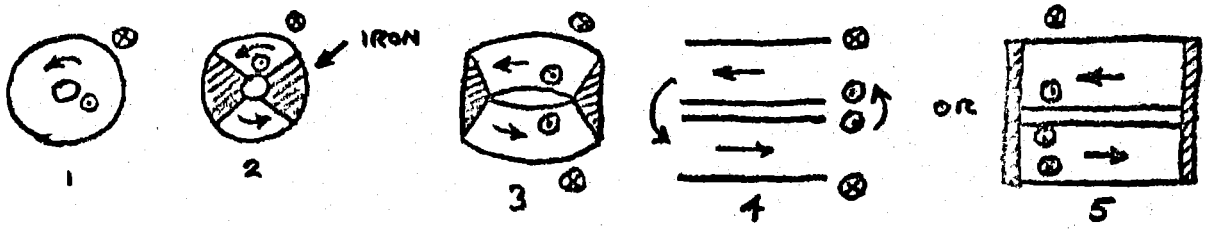

3) Uniform-field quadrupole: This design in its fully-developed form is two-dimensional, the third dimension being free to choose and depending only on cost and available power. Since it is topologically identical to (2), it does not link the storage ring vacuum chamber, and could be made as separate upper and lower halves, which could be removed or replaced without breaking the storage-ring vacuum. That fact may be quite important because of the desirability of full preparation of an experiment in advance of its installation at the ring, and of minimum down-time for other experiments at the storage-ring. In case some major repair or redesign becomes necessary after initial operation of the detector, it will also be quite important to be able to remove the entire apparatus without major disruption of the schedule for other experiments. Photography is relatively simple in this design and can be done with a single camera, which can be far from the high-radiation area near the ring. The first-view distance is minimal in this geometry, and there are no excessive current-densities. The magnetic field is uniform, which is a considerable convenience. The major disadvantage of the design is that it has low analysing power for particles of azimuthal angle close to the median plane; a version in which the distortion is stopped short of the full development to two-dimensionality would be free of that disadvantage, but would not have uniform field:

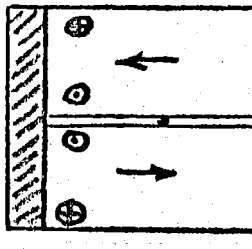

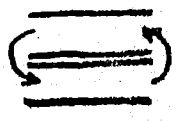

ANALYSING POWER AS A FUNCTION OF AZIMUTHAL ANGLE -

In the limit of thin current sheets, and with a thin vacuum chamber window over a wide azimuthal angle, the multiple scattering before arrival of a particle at the first-view point can be neglected. In that

approximation one can look at the dependence of momentum resolution on azimuthal angle in a fully-developed geometry (3). All designs which cover more than about 2/3 of the azimuthal angle will require more than one photographic view, so questions of stereo angle will not arise in this discussion:

Consider tracks with polar angle 90 degrees. The component of momentum transverse to the magnetic field B is

$p_t = p\sin\phi$, and the radius of curvature is $R = p_t/B$. Then the sagitta is $x = Y^2/2R = \text{const.}\ (Y^2/\sin\phi)$ for constant p/B. Then for constant sagitta error Δx the error in momentum p_t, and therefore in p also, is $\Delta p/p \sim \sin\phi/Y^2$. Where Y is limited by the termination of the magnetic field, the error goes as $1/\sin\phi$, but if the geometry is continued along the field axis the error goes as $\sin\phi$, actually decreasing at small ϕ. The azimuthal acceptance with good resolution can be made as large as desired at the expense of additional Aluminum and power.